

Redefinition of thérèsemaganite, $\text{NaCo}_4(\text{SO}_4)(\text{OH})_6\text{Cl}\cdot 6\text{H}_2\text{O}$: new data and relationship to ‘cobaltogordaite’

ANATOLY V. KASATKIN^{1,*}, JAKUB PLÁŠIL², RADEK ŠKODA³, DMITRIY I. BELAKOVSKIY¹, JOE MARTY⁴, NICOLAS MEISSER⁵ AND IGOR V. PEKOV⁶

¹ Fersman Mineralogical Museum of the Russian Academy of Sciences, Leninsky Prospekt 18-2, 119071 Moscow, Russia

² Institute of Physics ASCR, v.v.i., Na Slovance 2, 18221 Praha, Czech Republic

³ Department of Geological Sciences, Faculty of Science, Masaryk University, Kotlářská 2, CZ-611 37 Brno, Czech Republic

⁴ 5199 E Silver Oak Rd., Salt Lake City, UT 84108, USA

⁵ Musée Cantonal de Géologie, University of Lausanne, Building Anthropole, CH-1015 Lausanne, Switzerland

⁶ Faculty of Geology, Moscow State University, Vorobievsky Gory, 119991 Moscow, Russia

[Received 25 January 2017; Accepted 26 April 2017; Associate Editor: Stuart Mills]

ABSTRACT

Thérèsemaganite was originally described from the Cap Garonne mine, Var, France. Its ideal formula was reported as $(\text{Co,Zn,Ni})_6(\text{SO}_4)(\text{OH})_{10}\cdot 8\text{H}_2\text{O}$; without crystal structure data, only the powder X-ray diffraction pattern was given. Revision of the holotype material revealed that thérèsemaganite is identical to ‘cobaltogordaite’ (IMA2014-043), recently described from the Blue Lizard mine, Utah, USA. Thérèsemaganite is thus redefined in accordance with the new data obtained for the neotype specimen from Blue Lizard (formerly the holotype specimen of ‘cobaltogordaite’) and ‘cobaltogordaite’ has been discredited by the International Mineralogical Association Commission on New Mineral Nomenclature and Classification (IMA CNMNC). Thérèsemaganite has the ideal, end-member formula $\text{NaCo}_4(\text{SO}_4)(\text{OH})_6\text{Cl}\cdot 6\text{H}_2\text{O}$. The empirical formulae of the holotype (Cap Garonne) and the neotype (Blue Lizard), both based on microprobe analyses and calculated on the basis of 17 O + Cl atoms per formula unit (with fixed 6 OH groups and 6 H₂O molecules; H content is calculated by stoichiometry) are $(\text{Na}_{0.64}\text{K}_{0.09})_{\Sigma 0.73}(\text{Co}_{2.35}\text{Zn}_{1.22}\text{Ni}_{0.50})_{\Sigma 4.07}\text{S}_{1.02}\text{O}_{3.98}(\text{OH})_6\text{Cl}_{1.02}\cdot 6\text{H}_2\text{O}$ and $\text{Na}_{1.01}(\text{Co}_{1.90}\text{Zn}_{1.37}\text{Ni}_{0.48}\text{Cu}_{0.15}\text{Mn}_{0.05})_{\Sigma 3.95}\text{S}_{1.03}\text{O}_{4.09}(\text{OH})_6\text{Cl}_{0.91}\cdot 6\text{H}_2\text{O}$, respectively. Thérèsemaganite is trigonal, $P\bar{3}$, $a = 8.349(3)$, $c = 13.031(2)$ Å, $V = 786.6(4)$ Å³ and $Z = 2$ (neotype). The strongest powder X-ray diffraction lines are [d_{obs} in Å (hkl) (I_{rel}): 13.10 (001)(100), 6.53 (002)(8), 4.173 (110)(4), 3.517 (112)(5), 2.975 (104, 10 $\bar{4}$)(4), 2.676 (211)(5) and 2.520 (122)(5) (neotype). Thérèsemaganite is a cobalt analogue of gordaite, $\text{NaZn}_4(\text{SO}_4)(\text{OH})_6\text{Cl}\cdot 6\text{H}_2\text{O}$. These minerals represent the gordaite group, accepted by the IMA CNMNC.

KEYWORDS: thérèsemaganite, ‘cobaltogordaite’, redefinition, sodium cobalt sulfate, X-ray diffraction, gordaite group, oxidation zone, Cap Garonne mine, Blue Lizard mine.

Introduction

THÉRÈSEMAGANITE (IMA1991-026) was originally described as a new cobalt–zinc–nickel sulfate from the Cap Garonne mine, Var, Provence-Alpes-Côte

d’Azur, France. The characterization of the new species included electron probe analysis, powder X-ray diffraction (PXRD) and data on physical and optical properties. Due to the nature of the material (very thin plates forming spherules) single-crystal X-ray diffraction studies could not be carried out. The unit-cell parameters were calculated from PXRD data by the Ito method and thérèsemaganite was reported to be hexagonal, with an unknown

*E-mail: anatoly.kasatkin@gmail.com

<https://doi.org/10.1180/minmag.2017.081.030>

space group, having parameters of $a = 8.363(8)$, $c = 26.18(7)$ Å, $V = 1586(3)$ Å³ and $Z = 3$. Its ideal chemical formula was reported as $(\text{CoZnNi})_6(\text{SO}_4)(\text{OH}, \text{Cl})_{10} \cdot 8\text{H}_2\text{O}$ (Sarp, 1993).

More recently, our research team discovered at the Blue Lizard mine, San Juan Co., Utah, USA, a mineral that turned out to be the cobalt analogue of gordaite, $\text{NaZn}_4(\text{SO}_4)(\text{OH})_6\text{Cl} \cdot 6\text{H}_2\text{O}$, described by Schlüter *et al.* (1997). The new species with the name ‘cobaltogordaite’ and the ideal formula $\text{NaCo}_4(\text{SO}_4)(\text{OH})_6\text{Cl} \cdot 6\text{H}_2\text{O}$ was submitted to the IMA CNMNC and subsequently approved under the code IMA2014-043 (Kasatkin *et al.*, 2014). However, during preparation of the paper for its detailed description, it was found that some characteristics of ‘cobaltogordaite’ are very close to those of thèrèsemaganite. In particular, both species showed similar PXRD patterns, optical data, physical and chemical properties. The unit-cell parameters of thèrèsemaganite differed from that of ‘cobaltogordaite’ by a doubled c axis, but, as mentioned above, they were only calculated from PXRD data, while single-crystal studies were lacking. At the same time, the chemical composition of thèrèsemaganite and ‘cobaltogordaite’ differed considerably, for example: there are the absence of Na in the former and different amounts of OH, Cl and H₂O caused a different stoichiometry. Such a chemical difference was the main reason why we initially proposed ‘cobaltogordaite’ as a separate mineral species to the IMA. In the paper by Sarp (1993) no details were given on the conditions used for the electron microprobe analysis (EMPA). As thèrèsemaganite contains a significant amount of Zn, and the spectral lines $\text{ZnL}\alpha, \beta$ and $\text{NaK}\alpha$ are in complete overlap in the energy-dispersive spectrum (EDS), it was suggested that Na could have been missed and, as a result, the formula of thèrèsemaganite might be wrong.

We decided then to restudy the type material of thèrèsemaganite in order to compare it with ‘cobaltogordaite’. We were able to obtain a few tiny grains from the holotype specimen of thèrèsemaganite (registration number 477.078) from Muséum d’Histoire Naturelle et Musée d’Histoire des Sciences, Geneva, Switzerland. Unfortunately, the extremely small quantity and imperfectness of the material precluded the complete reinvestigation of this mineral. The single-crystal X-ray diffraction experiment did not provide any satisfactory data. As the most important point was the difference in chemical compositions of thèrèsemaganite and ‘cobaltogordaite’, we concentrated our efforts on EMPA. A careful microprobe study of the holotype material revealed that

thèrèsemaganite, indeed, contains sodium and that thèrèsemaganite and ‘cobaltogordaite’ are chemically identical. Further comparison of the data given by Sarp (1993) with our data for ‘cobaltogordaite’ left no doubts that thèrèsemaganite and ‘cobaltogordaite’ are the same mineral species. This conclusion led us to submit the proposal on redefinition of thèrèsemaganite to the IMA CNMNC. The name thèrèsemaganite was retained as having priority while the name ‘cobaltogordaite’ was withdrawn. The type specimen of ‘cobaltogordaite’ deposited in the collections of the Fersman Mineralogical Museum of the Russian Academy of Sciences, Moscow, Russia, under registration number 4561/1 and catalogued in the systematic collection of the Museum under inventory number 94617, was designated as the neotype specimen of thèrèsemaganite. The redefinition of thèrèsemaganite based on the neotype and the formal discreditation of ‘cobaltogordaite’ have been approved by the IMA CNMNC in September 2015, proposal 15-K (Hålenius *et al.*, 2015). This paper represents a detailed report on the redefinition of thèrèsemaganite with new data for this mineral including its crystal structure determination carried out on the neotype.

Occurrence and paragenesis

At its type locality, the abandoned copper mine Cap Garonne, Var, Provence-Alpes-Côte d’Azur, France (43°4’53”N, 6°1’55”E), thèrèsemaganite occurs deeply in Triassic conglomerate inside the intergranular space of quartz (Favreau and Galéa-Clolus, 2014). Sarp (1993) mentions association with guarinoite, anglesite, antlerite, Co- and Ni-bearing ktenasite, cerussite, brochantite, rutile, covellite, tennantite and gersdorffite. The above association also includes malachite and a potentially new copper sulfate, currently under investigation (Georges Favreau, pers. comm.). A detailed description of the mine, its history, geology and mineralogy is given by Favreau and Galéa-Clolus (2014).

At the neotype locality, the abandoned uranium mine Blue Lizard, White Canyon District, San Juan Co., Utah, USA (37°33’26”N, 110°17’48”W), thèrèsemaganite occurs as a secondary mineral originating from the post-mining weathering processes such as oxidation of primary sulfides that permeate Triassic sandstones and siltstones (Thaden *et al.*, 1964). Thèrèsemaganite is one of the numerous sulfates formed in the humid underground environment as efflorescent crusts on the

surface of mine walls and tunnels. The regular collecting efforts undertaken at the Blue Lizard mine by one of the authors (JM) within last few years has revealed an incredibly rich supergene mineralization and resulted in the discovery and description of a series of new mineral species all of which, so far, are sulfates alwilkinsite-(Y), belakovskiite, bluelizardite, bobcookite, chinleyite-(Y), cobaltoblödite, fermiite, klaprothite, manganoblödite, meisserite, oppenheimerite, ottohahnite, péligotite, plášilite, redcanyonite and wetherillite. A detailed description of the mine, its history and geology are provided by Thaden *et al.* (1964), Chenoweth (1993) and Kampf *et al.* (2015).

The neotype specimen of thérèsemagnanite was collected in October 2013 by one of the authors (JM). The mineral occurs on sandstone matrix consisting of irregular quartz grains and is closely associated with alpersite, anhydrite, calcite, dickite, epsomite, gypsum, haydeecite, hexahydrate, natrozippeite, paratacamite and tamarugite. In other samples from Blue Lizard thérèsemagnanite is associated also with Co-rich gordaite forming a solid-solution series with the latter.

General appearance, physical properties and optical data

According to Sarp (1993), thérèsemagnanite from Cap Garonne occurs as pink to light pink radiated spherulites (up to 0.2 mm in diameter) consisting of very thin platy crystals (Fig. 1). They are transparent, with pearly lustre and light pink streak; they are very soft and very fragile with uneven fracture. The mineral does not fluoresce. Cleavage on {001} is perfect.



FIG. 1. Light-pink platy crystals of thérèsemagnanite with green crystals of a potentially new copper sulfate. Cap Garonne mine (the holotype specimen). Field of view: width: 1.3 mm. Photo: Pierre Clolus.

In the neotype specimen thérèsemagnanite forms well-shaped, lamellar, hexagonal crystals up to 0.1 mm in size, but usually much smaller, typically split and forming rose-like clusters up to 0.2 mm across (Fig. 2 and 3). Some crystals are coarse and twisted. It is pink in colour, transparent and has a white streak and vitreous lustre. It shows no fluorescence in ultraviolet radiation or when exposed to the cathode rays. It is sectile, has a laminated fracture and a perfect cleavage on {001}. The Mohs' hardness is estimated at 2½.

The density of thérèsemagnanite from Cap Garonne measured in heavy liquids is 2.52(2) g cm⁻³ and the calculated density is 2.48(1) g cm⁻³ (Sarp, 1993). An extremely small quantity of available material from Blue Lizard mine precluded the direct measurement of its density. The calculated density based on the empirical formula is 2.557 g cm⁻³.

Optically, thérèsemagnanite from France is uniaxial negative; the refractive indices at 590 nm are: $\omega = 1.568(2)$ and $\epsilon = 1.542(2)$. The pleochroism is intense with $O = \text{pink}$ and $E = \text{light pink}$ to colourless (Sarp, 1993). Thérèsemagnanite from



FIG. 2. Pink clusters of thérèsemagnanite crystals with whitish gypsum on sandstone. Blue Lizard mine (the neotype specimen). Field of view: width: 0.8 mm. Photo: Tim Pashko.

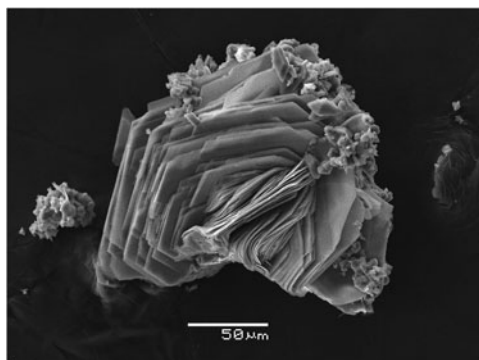


FIG. 3. Rose-like cluster of lamellar hexagonal thèrèsemagnanite crystals from the Blue Lizard mine (the neotype specimen). Scanning electron microscope (secondary electron) image.

USA is optically biaxial (–) (most likely anomalously biaxial due to the deformation of the twisted crystals). The refractive indices are: $\alpha = 1.547(3)$ and $\beta = \gamma = 1.570(3)$ ($\lambda = 589$ nm). $2V$ was measured by conoscopical observations by rotating grains on a self-made spindle stage and is $10(5)^\circ$. In transmitted light thèrèsemagnanite from Blue Lizard is transparent, pale pink in thicker grains to colourless in thin grains. Dispersion of optical axes is weak, $r < v$. Compared to the French material, thèrèsemagnanite from the USA is very weakly pleochroic in pale pink tones with $X > Y \sim Z$ (pleochroism is visible only in thicker grains); X is perpendicular to (001).

Thèrèsemagnanite from both localities is soluble in 10% HCl. Additional chemical tests performed on thèrèsemagnanite from the neotype locality showed it to be slowly soluble in hot water and rapidly dissolved in cold 30% HNO_3 .

Chemical data

As noted before, the composition was a key point in proving the identity of thèrèsemagnanite from Cap Garonne mine with the mineral from the Blue Lizard mine initially investigated by us.

Chemical data for the neotype specimen (Table 1) were obtained using a CamScan 4D scanning electron microscope equipped with an Oxford Link ISIS energy-dispersive X-ray spectrometer. Operating conditions were as follows: voltage 12 kV, beam current 500 pA and beam rastered on an area 8×8 μm in order to minimize

sample damage. The following standards were used: chkalovite (Na), MnTiO_3 (Mn), Co metal (Co), NiO (Ni), Cu metal (Cu), ZnO (Zn), BaSO_4 (S) and HgCl (Cl). Special attention was paid to the accuracy of the resolution between the $\text{NaK}\alpha$ and $\text{ZnL}\alpha$ analytical lines during measurement of Na, while Zn content was measured using the $\text{ZnK}\alpha$ line.

No other elements with atomic numbers >8 were detected. The content of H_2O was not determined directly because of the scarcity of pure available material. The H_2O content was calculated by stoichiometry, with 6 H_2O molecules per formula unit, according to the structure data for gordaite-group minerals. The Raman spectrum (see below) confirmed the presence of H_2O molecules and O–H bonds belonging to OH groups and, at the same time, showed the absence of B–O, C–O and N–O bonds in the mineral.

The two polycrystalline grains of thèrèsemagnanite (each ~ 30 μm across) removed from the holotype specimen were mounted into epoxy resin, polished and analysed using a CAMECA SX100 electron-probe microanalyser (accelerating voltage of 15 kV, a beam current of 4 nA and a beam diameter of 5 μm). The defocused beam was used to minimize damage to the analysed area under the electron beam. The very poor quality of the thèrèsemagnanite holotype material and tiny size of the aggregates did not allow us to use a broader beam. The following standards were used: albite (Na), sanidine (K), Co metal (Co), Ni_2SiO_4 (Ni), gahnite (Zn), SrSO_4 (S) and vanadinite (Cl). The raw data were processed using the X-phi matrix correction routine (Merlet, 1994).

Despite lowering the energy of the electron beam (compared to conditions applied during routine EMPA) the holotype thèrèsemagnanite was found to be very prone to fast dehydration and volatilization of Na, which led also to quite low analytical totals. Only three points with appropriate results were collected before the mineral entirely decomposed. This effect was noticed by previous researchers of similar minerals. Nasdala *et al.* (1998) stated that during their attempts to analyse the chemistry of gordaite using the wavelength dispersive spectroscopy mode, even with the lowest possible current beam, the mineral bubbled and degassed within a few seconds of exposure to electron beam.

The chemical composition obtained for both holotype and neotype material along with the original data of Sarp (1993) is given in Table 1.

TABLE 1. Chemical composition of thérèsemagnanite (electron microprobe data).

| Constituent | Holotype, Cap Garonne mine (Sarp, 1993) | | | Holotype, Cap Garonne mine (our data, mean of 3 analyses) | | | Normalized wt.% | Neotype, Blue Lizard mine (our data, mean of 8 analyses) | | |
|-------------------|--|-------------|-----|--|-------------|------|-----------------|---|-------------|------|
| | wt.% | Range | SD | wt.% | Range | SD | | wt.% | Range | SD |
| Na ₂ O | – | – | – | 2.55 | 1.47–2.91 | 0.62 | 3.24 | 5.25 | 4.17–6.31 | 0.74 |
| K ₂ O | – | – | – | 0.54 | 0.26–1.37 | 0.47 | 0.69 | – | – | – |
| MnO | – | – | – | – | – | – | – | 0.54 | 0.38–0.73 | 0.12 |
| CoO | 32.95 | 32.12–33.57 | 0.6 | 22.78 | 17.55–24.53 | 2.98 | 28.90 | 23.98 | 19.53–27.58 | 2.77 |
| NiO | 3.18 | 2.77–3.50 | 0.3 | 4.88 | 4.59–4.98 | 0.16 | 6.19 | 6.03 | 4.40–7.09 | 1.00 |
| CuO | 0.16 | 0.06–0.23 | 0.6 | – | – | – | – | 1.95 | 1.25–2.81 | 0.63 |
| ZnO | 20.42 | 19.95–21.55 | 0.6 | 12.90 | 8.71–14.34 | 2.40 | 16.37 | 18.72 | 16.43–21.99 | 2.03 |
| SO ₃ | 10.54 | 10.35–10.73 | 0.2 | 10.53 | 7.72–11.47 | 1.60 | 13.36 | 13.91 | 11.73–15.52 | 1.40 |
| Cl | 5.65 | 5.08–6.05 | 0.4 | 4.69 | 3.14–5.21 | 0.88 | 5.95 | 5.41 | 4.88–5.99 | 0.51 |
| H ₂ O* | 28.40 | | | 21.00 | | | 26.64 | 27.27 | | |
| O=Cl | –1.28 | | | –1.06 | | | –1.34 | –1.22 | | |
| Total | 100.02 | | | 78.81 | | | 100 | 101.84 | | |

SD = standard deviation; – = content of a constituent below detection limit; * calculated by stoichiometry.

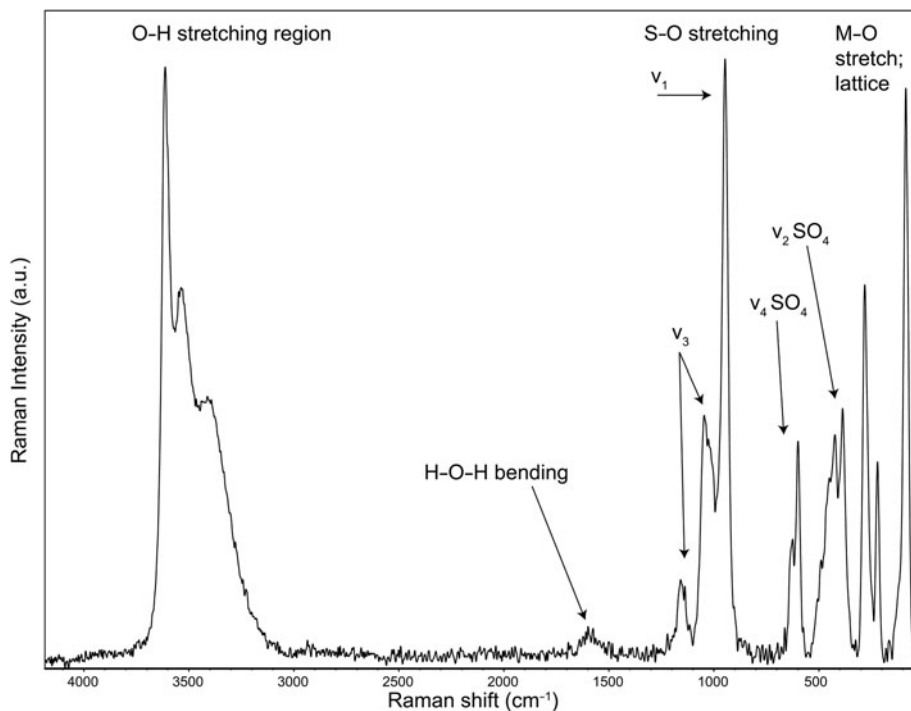


FIG. 4. The Raman spectrum of thèrèsemaganite from the Blue Lizard mine (the neotype specimen).

The empirical formulae of the holotype specimen from Cap Garonne and the neotype specimen from Blue Lizard, both based on EMPA and calculated on the basis of 17 O + Cl atoms per formula unit (with fixed 6 OH groups and 6 H₂O molecules), are $(\text{Na}_{0.64}\text{K}_{0.09})_{\Sigma 0.73}(\text{Co}_{2.35}\text{Zn}_{1.22}\text{Ni}_{0.50})_{\Sigma 4.07}\text{S}_{1.02}\text{O}_{3.98}(\text{OH})_6\text{Cl}_{1.02}\cdot 6\text{H}_2\text{O}$ and $\text{Na}_{1.01}(\text{Co}_{1.90}\text{Zn}_{1.37}\text{Ni}_{0.48}\text{Cu}_{0.15}\text{Mn}_{0.05})_{\Sigma 3.95}\text{S}_{1.03}\text{O}_{4.09}(\text{OH})_6\text{Cl}_{0.91}\cdot 6\text{H}_2\text{O}$, respectively.

Despite all the above mentioned analytical problems, our data clearly show that the holotype of thèrèsemaganite contains Na missed by Sarp (1993), most probably due to overlap of ZnL α , β and NaK α lines. The overall stoichiometry of thèrèsemaganite from Cap Garonne mine is also distinct from that reported by Sarp (1993) and is, in fact, identical with that of the material from the Blue Lizard mine.

The ideal formula of thèrèsemaganite is, thus, $\text{NaCo}_4(\text{SO}_4)(\text{OH})_6\text{Cl}\cdot 6\text{H}_2\text{O}$, which requires Na₂O 5.16, CoO 49.94, SO₃ 13.33, Cl 5.91 and H₂O 27.00, O = Cl -1.34, total 100 wt.%.

The Gladstone-Dale compatibility index for the neotype specimen is 0.024, rated as excellent (Mandarino, 1981).

Raman spectroscopy

The Raman spectrum (Fig. 4) of a thèrèsemaganite crystal aggregate (neotype specimen) was collected using a DXR dispersive Raman spectrometer mounted on a confocal Olympus microscope and acquired in the range 50–6400 cm⁻¹ (spectral resolution of 5 cm⁻¹). The Raman signal was excited by a 532 nm laser and detected by a CCD detector. Experimental conditions were: exposure time, 10 s; number of exposures, 64; grating, 400 lines mm⁻¹; spectrograph aperture, 50 μm pinhole; and a laser power level of 2.0 mW. We carried out our assignments of the Raman spectrum of thèrèsemaganite following Lane (2007).

The Raman spectrum is dominated by O–H and S–O stretching and bending vibrations. The O–H stretching modes occur between 3610 and 3400 cm⁻¹. According to the empirical correlation given by Libowitzky (1999), O \cdots O separation distances of the corresponding Hbonds are expected to be in the range 2.8–3.1 Å, which is very similar with respect to the values for hydrogen bond lengths in gordaite given by Adiwidjaja *et al.* (1997). The H–O–H (ν_2) bending vibrations occur

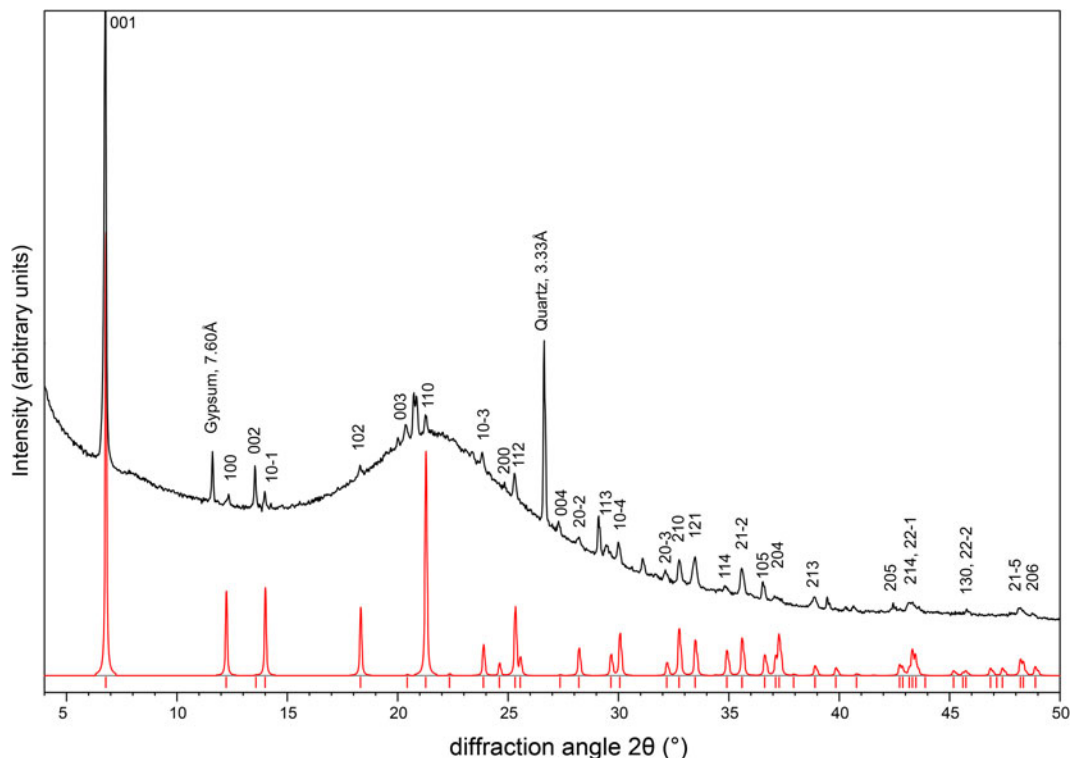


Fig. 5. Comparison of the observed powder X-ray diffraction profile and calculated PXRD pattern based on the structure model of Adiwidjaja *et al.* (1997).

at 1600 cm^{-1} . Split SO_4 vibrations (ν_3) occur at 1220 , 1160 and 1045 cm^{-1} , and the symmetric stretching vibration (ν_1) of SO_4 at 945 cm^{-1} . Bands at 625 and 600 and at 425 and 390 cm^{-1} were assigned to bending modes (ν_4 and ν_2 , respectively) of SO_4 tetrahedra. Bands below 390 cm^{-1} can be related to low-energy lattice modes, in particular modes involving Co–O and Zn–O stretching vibrations.

X-ray crystallography and crystal structure

A crystal aggregate of thérèsemagnanite from the Blue Lizard mine, with dimensions of $0.10\text{ mm} \times 0.08\text{ mm} \times 0.02\text{ mm}$, composed of several thin, intimately intergrown crystals, was examined using an Oxford Diffraction Gemini single-crystal diffractometer with an Atlas CCD detector utilizing monochromatized $\text{MoK}\alpha$ radiation (at 50 kV , 35 mA). The unit cell was refined from 171 individual reflections by the least-squares algorithm of the *CrysAlis* software (Oxford Diffraction, Oxford, UK) with the following trigonal unit-cell

parameters: $a = 8.345(6)$, $c = 13.06(3)\text{ \AA}$, $V = 787.6(2)\text{ \AA}^3$ and $Z = 2$.

Due to the above mentioned findings, we attempted to refine the structure of thérèsemagnanite by means of the Rietveld refinement from PXRD data. Data were collected using a PANalytical Empyrean powder diffractometer equipped with a Cu X-ray tube and a PIXcel^{3D} solid-state detector. Data were collected in the Debye-Scherrer geometry over the range of 3 to $90^\circ 2\theta$ with a step size of $0.028^\circ 2\theta$ and a total counting time of 48 hours spent accumulating 40 scans, which were merged then to improve the intensity statistics. Less than 0.1 mg of material was available for the powder study, which resulted in a dataset of limited quality, not suitable for conventional Rietveld analysis. Therefore, only a comparison of the observed powder profile and theoretical powder pattern calculated (*PowderCell* program; Kraus and Nolze, 1996) using the model of Adiwidjaja *et al.* (1997) is given in Fig. 5. Powder X-ray data (in \AA for $\text{CuK}\alpha$) are listed in Table 2. Powder data are affected, due to a very limited volume of the mineral used for the

TABLE 2. Powder X-ray diffraction data for thérèsemaganite.

| Holotype, Cap Garonne mine (Sarp, 1993) | | | | | | Neotype, Blue Lizard mine | | | | | | |
|--|------------------|-------------------|-----|-----|-----|---------------------------|------------------|-------------------|-------------------|-----|-----|-----------|
| I_{obs} | d_{obs} | d_{calc} | h | k | l | I_{obs} | d_{obs} | I_{calc} | d_{calc} | h | k | l |
| 100 | 13.1 | 13.090 | 0 | 0 | 2 | 100 | 13.10 | 100 | 13.03 | 0 | 0 | 1 |
| | | | | | | 2 | 7.18 | 21 | 7.23 | 1 | 0 | 0 |
| 25 | 6.552 | 6.545 | 0 | 0 | 4 | 8 | 6.53 | <1 | 6.51 | 0 | 0 | 2 |
| 10 | 6.330 | 6.337 | 1 | 0 | 2 | 3 | 6.329 | 19 | 6.322 | 1 | 0 | $\bar{1}$ |
| | | | | | | 2 | 4.846 | 15 | 4.840 | 1 | 0 | 2 |
| 5 | 4.371 | 4.363 | 0 | 0 | 6 | 3 | 4.358 | <1 | 4.343 | 0 | 0 | 3 |
| 25 | 4.177 | 4.182 | 1 | 1 | 0 | 4 | 4.173 | 55 | 4.175 | 1 | 1 | 0 |
| 5 | 3.742 | 3.737 | 1 | 0 | 6 | 3 | 3.731 | 9 | 3.723 | 1 | 0 | $\bar{3}$ |
| 30 | 3.523 | 3.524 | 1 | 1 | 4 | 5 | 3.517 | 10 | 3.515 | 1 | 1 | 2 |
| | | | | | | 2 | 3.265 | <1 | 3.257 | 0 | 0 | 4 |
| | | | | | | 2 | 3.162 | 8 | 3.161 | 2 | 0 | $\bar{2}$ |
| | | | | | | 2 | 3.028 | 5 | 3.010 | 1 | 1 | 3 |
| | | | | | | | | 3 | 3.010 | 1 | 1 | $\bar{3}$ |
| 30 | 2.985 | 2.982 | 1 | 0 | 8 | 4 | 2.975 | 6 | 2.970 | 1 | 0 | 4 |
| | | | | | | | | 9 | 2.970 | 1 | 0 | $\bar{4}$ |
| | | | | | | 2 | 2.782 | 3 | 2.779 | 2 | 0 | 3 |
| 25 | 2.736 | 2.737 | 2 | 1 | 0 | 4 | 2.731 | 8 | 2.733 | 1 | 2 | 0 |
| | | | | | | | | 10 | 2.733 | 2 | 1 | 0 |
| 40 | 2.681 | 2.679 | 1 | 2 | 2 | 5 | 2.676 | 1 | 2.675 | 2 | 1 | 1 |
| | | | | | | 1 | 2.571 | 4 | 2.568 | 1 | 1 | 4 |
| | | | | | | | | 6 | 2.568 | 1 | 1 | $\bar{4}$ |
| 90 | 2.527 | 2.525 | 1 | 2 | 4 | 5 | 2.520 | 5 | 2.520 | 1 | 2 | 2 |
| | | | | | | 3 | 2.455 | 2 | 2.451 | 2 | 0 | 4 |
| | | | | | | | | 4 | 2.451 | 2 | 0 | $\bar{4}$ |
| 20 | 2.329 | { 2.319 | 1 | 2 | 6 | 1 | 2.422 | 13 | 2.420 | 3 | 0 | 0 |
| | | { 2.327 | 3 | 0 | 3 | 1 | 2.404 | 2 | 2.410 | 1 | 2 | 3 |
| | | | | | | 2 | 2.315 | 1 | 2.313 | 1 | 1 | 5 |
| | | | | | | 1 | 2.217 | 1 | 2.210 | 1 | 2 | 4 |
| | | | | | | | | 1 | 2.210 | 1 | 2 | $\bar{4}$ |
| | | | | | | 1 | 2.095 | 9 | 2.094 | 2 | 2 | 0 |
| 10 | 2.104 | { 2.112 | 3 | 0 | 6 | 1 | 2.085 | 2 | 2.087 | 1 | 0 | 6 |
| | | { 2.100 | 1 | 2 | 8 | | | 2 | 2.087 | 1 | 0 | $\bar{6}$ |
| | | | | | | 1 | 2.073 | 2 | 2.080 | 3 | 1 | 0 |
| 5 | 1.894 | 1.892 | 1 | 2 | 10 | 1 | 1.889 | 1 | 1.886 | 2 | 2 | 3 |
| | | | | | | | | 2 | 1.886 | 2 | 2 | $\bar{3}$ |
| | | | | | | 1 | 1.884 | 1 | 1.881 | 1 | 0 | 7 |
| | | | | | | | | 2 | 1.881 | 1 | 0 | $\bar{7}$ |
| | | | | | | 2 | 1.798 | 2 | 1.802 | 1 | 3 | 4 |
| | | | | | | | | 2 | 1.802 | 1 | 3 | $\bar{4}$ |
| 10 | 1.711 | 1.712 | 1 | 3 | 8 | 2 | 1.704 | 1 | 1.708 | 1 | 2 | 6 |
| | | | | | | 1 | 1.693 | 1 | 1.700 | 4 | 0 | $\bar{3}$ |
| 20 | 1.576 | { 1.580 | 4 | 1 | 0 | 1 | 1.577 | 2 | 1.578 | 1 | 4 | $\bar{1}$ |
| | | { 1.578 | 4 | 1 | 1 | | | | | | | |
| 10 | 1.546 | { 1.555 | 4 | 1 | 3 | | | | | | | |
| | | { 1.553 | 3 | 2 | 6 | | | | | | | |
| | | { 1.546 | 3 | 0 | 13 | $\bar{1}$ | 1.400 | 1 | 1.399 | 5 | 0 | 3 |

analysis, by the preferred orientation of plate-like crystallites, strongly enhancing intensities of the 00/ reflections. The fact that this aberration appeared can

be easily explained due to the small amount of the powder in the capillary used for the experiment and the plate-like crystallites stacked to the wall of the

TABLE 3. Comparative data for thérèsemagnanite (holotype and neotype = ‘cobaltgordaite’) and gordaite.

| Mineral | Thérèsemagnanite holotype | Thérèsemagnanite neotype (formerly ‘cobaltgordaite’) | Gordaite |
|-----------------------------|--|--|---|
| End-member formula | NaCo ₄ (SO ₄)(OH) ₆ Cl·6H ₂ O* | | NaZn ₄ (SO ₄)(OH) ₆ Cl·6H ₂ O |
| Empirical formula | (Na _{0.64} K _{0.09}) _{Σ0.73} (Co _{2.35} Zn _{1.22} Ni _{0.50}) _{Σ4.07} S _{1.02} O _{3.98} (OH) _{6.00} Cl _{1.02} ·6H ₂ O* | Na _{1.01} (Co _{1.90} Zn _{1.37} Ni _{0.48} Cu _{0.15} Mn _{0.05}) _{Σ3.95} S _{1.03} O _{4.09} (OH) ₆ Cl _{0.91} ·6H ₂ O | Na _{1.54} Zn _{3.39} (SO ₄)(OH) ₆ Cl _{0.95} ·6H ₂ O |
| Crystal system | Trigonal | Trigonal | Trigonal |
| Space group | <i>P</i> 3 | <i>P</i> 3 | <i>P</i> 3 |
| <i>a</i> , Å | 8.363(8) | 8.349(3) | 8.3556(3) |
| <i>c</i> , Å | 13.09(4)** | 13.031(2) | 13.025(1) |
| <i>V</i> , Å ³ | 793(2)** | 786.6(4) | 787.54(8) |
| <i>Z</i> | 2 | 2 | 2 |
| Strongest lines | 13.10–100 | 13.10–100 | 12.950–100 |
| of the powder X-ray | 6.552–25 | 6.53–8 | 6.501–23 |
| diffraction | 4.177–25 | 4.173–4 | 4.339–15 |
| pattern: | 3.523–30 | 3.517–5 | 3.258–14 |
| <i>d</i> , Å – <i>I</i> , % | 2.985–30 | 2.975–4 | 2.967–10 |
| | 2.736–25 | 2.731–4 | 2.676–5 |
| | 2.681–40 | 2.676–5 | 2.523–6 |
| | 2.527–90 | 2.520–5 | |
| Colour | Pink to light pink | Pink | Colourless to white |
| Morphology and size | Radiated spherules with diameter up to 0.2 mm made of very thin platy crystals | Rose-like clusters up to 0.2 mm across made of well-shaped lamellar hexagonal crystals | Flaky crystals up to 2 cm and masses of platy interlocked crystals |
| Lustre | Pearly | Vitreous | Vitreous to pearly |
| Cleavage | Perfect on {001} | Perfect on {001} | Perfect on {001} |
| Optical data | Uniaxial (–) ω = 1.568(2) ε = 1.542(2) | Biaxial (anomalously) (–) α = 1.547(3) β = 1.570(3) γ = 1.570(3) 2 <i>V</i> = 10(5) ^o (meas.) | Uniaxial (–) ω = 1.5607(8) ε = 1.5382(4) |
| Density | 2.52(2) (meas.) 2.48(1) (calc.) | none measured 2.557 (calc.) | 2.627 (meas.) 2.640 (calc.) |
| References | Sarp (1993); our data (marked with one asterisk) | Our data | Schlüter <i>et al.</i> (1997) |

* Our data for the holotype; ** calculated by us from the original data reported by Sarp (1993): *c* = 26.18(7) Å, *V* = 1586(3) Å³.

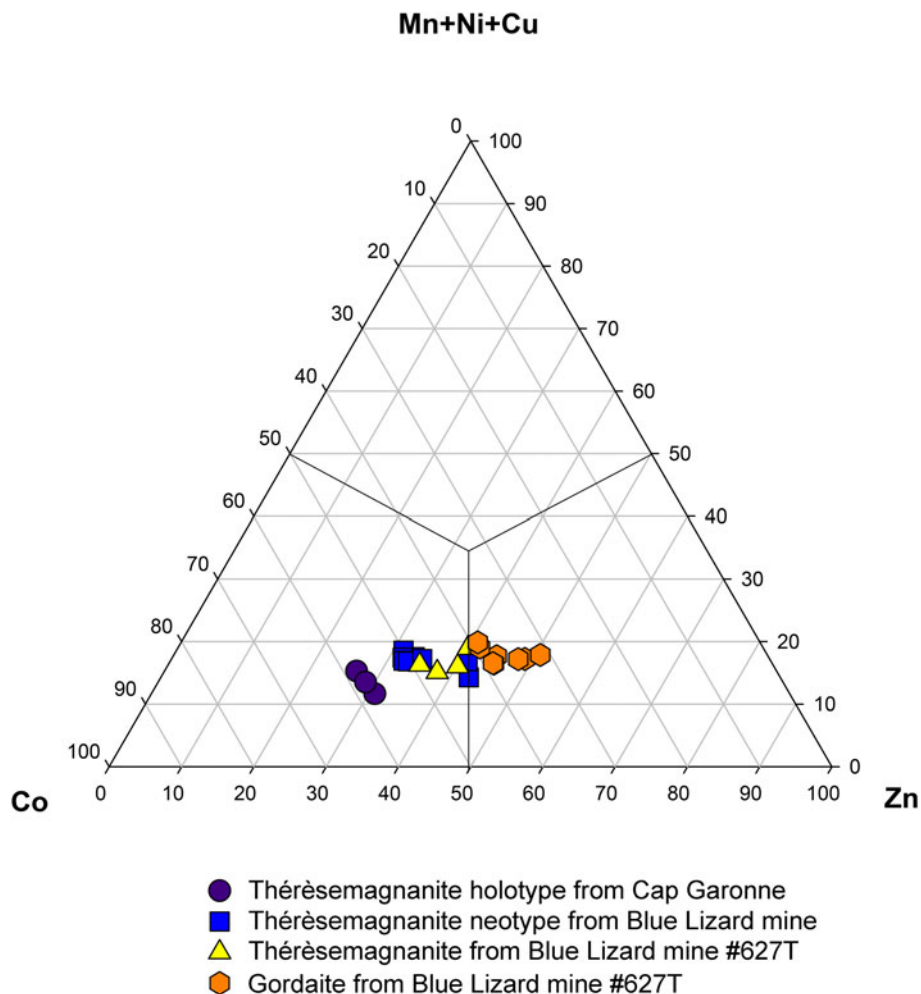


FIG. 6. A ternary plot showing the ratios of bivalent cations occupying M^{2+} sites in minerals of the thérèsemagnanite-gordaite series.

capillary by their prominent {001} crystal faces, due to the perfect cleavage on that pinacoid. That is why (002) or (004) diffractions were observed in the data. However, the observed pattern is similar to that of the calculated pattern from the structural model of gordaite, therefore we can assume that these two minerals are isostructural.

Relation to other species and nomenclature issues

Thérèsemagnanite is isostructural to its Zn-analogue gordaite, $\text{NaZn}_4(\text{SO}_4)(\text{OH})_6\text{Cl}\cdot 6\text{H}_2\text{O}$

(Schlüter *et al.*, 1997). According to the IMA CNMNC rules of the standardization of the mineral group hierarchies (Mills *et al.*, 2009), thérèsemagnanite and gordaite form the gordaite group. Even if thérèsemagnanite was described earlier, our choice of the group name is due to the fact that the structure of gordaite was solved first and gordaite had correct and complete data. The gordaite group has been approved by the IMA CNMNC, proposal 15-K (Hålenius *et al.*, 2015).

The comparison of chemistry, crystal data, optical and other physical properties for thérèsemagnanite (both holotype and neotype) and gordaite is given in Table 3.

At the Blue Lizard mine thérèsemagnanite specimens with different Co:Zn ratio were observed. While in the neotype sample (as well as the holotype material from Cap Garonne) all points of analyses showed the prevalence of Co over Zn, other specimens from Blue Lizard demonstrated an extended chemical diversity, yielding data that correspond to a thérèsemagnanite–gordaite solid-solution series. A good example is the sample #627 T from the collection of the senior author. The compositional variations within the series (for divalent cations occupying M^{2+} sites) are shown in Fig. 6. The corresponding cation compositions for the points that were analysed range from $(\text{Co}_{1.95}\text{Zn}_{1.39}\text{Ni}_{0.48}\text{Cu}_{0.13}\text{Mn}_{0.05})_{\Sigma 4.00}$ to $(\text{Zn}_{2.03}\text{Co}_{1.26}\text{Ni}_{0.44}\text{Cu}_{0.24}\text{Mn}_{0.03})_{\Sigma 4.00}$. For comparison, the point richest in Co found in the neotype specimen corresponds to $(\text{Co}_{2.03}\text{Zn}_{1.29}\text{Ni}_{0.53}\text{Cu}_{0.11}\text{Mn}_{0.04})_{\Sigma 4.00}$.

It is noteworthy that Nasdala *et al.* (1998) mention an existence of a copper-rich gordaite and its copper-dominant (in M^{2+}) analogue at the Kupferschiefer dump near the city of Helbra, Mansfeld region, Germany (51°33'23"N, 11°31'14"E). The distribution of the divalent cation positions is in the range from $(\text{Zn}_{2.1}\text{Cu}_{1.9})$ to $(\text{Cu}_{2.3}\text{Zn}_{1.7})$ leading, here as well, to a very probable existence of a solid solution between the Zn- and Cu-dominant species. The latter can be considered as a potentially new member of the gordaite group.

Acknowledgements

Reviewers Volker Kahlenberg and Georges Favreau, Structural Editor Peter Leverett and Editorial Board Member Stuart Mills are thanked for their useful suggestions and comments that helped us to improve the manuscript. The authors are grateful to Cédric Schnyder (Muséum d'Histoire Naturelle et Musée d'Histoire des Sciences, Geneva) who provided us with the fragments of the holotype specimen of thérèsemagnanite and to Pierre Clolus and Tim Pashko who helped with the photographs. Georges Favreau kindly provided additional information about associated minerals at Cap Garonne. Ladislav Lapčák and Atali A. Agakhanov are thanked for their assistance with Raman spectroscopic and microprobe analyses, respectively. We are indebted to Henrik Friis and Nikita V. Chukanov for their constructive criticism of our first draft of the 'cobaltogordaite' paper that turned our attention to the issue of thérèsemagnanite. This research was partially supported by the project of GACR 17-09161S to J.P.

References

- Adiwidjaja, G., Friese, K., Klaska, K.-H. and Schlüter, J. (1997) The crystal structure of gordaite $\text{NaZn}_4(\text{SO}_4)(\text{OH})_6\text{Cl}\cdot 6\text{H}_2\text{O}$. *Zeitschrift für Kristallographie*, **212**, 704–707.
- Chenoweth, W.L. (1993) *The geology and production history of the uranium deposits in the White Canyon mining district, San Juan County, Utah*. Miscellaneous Publication 93-3, Utah Geological Survey, Salt Lake City, Utah, USA.
- Favreau, G. and Galea-Clolus, V. (2014) *Cap Garonne*. Association Française de Microminéralogie, France, 320 pp.
- Hålenius, U., Hatert, F., Pasero, M. and Mills, S.J. (2015) IMA Commission on New Minerals, Nomenclature and Classification, Newsletter 27. New minerals and nomenclature modifications approved in 2015. *Mineralogical Magazine*, **79**(5), 1229–1236.
- Kampf, A.R., Plášil, J., Kasatkin, A.V. and Marty, J. (2015) Bobcookite, $\text{NaAl}(\text{UO}_2)_2(\text{SO}_4)_4(\text{H}_2\text{O})_{18}$, and wetherillite, $\text{Na}_2\text{Mg}(\text{UO}_2)_2(\text{SO}_4)_4\cdot 18\text{H}_2\text{O}$, two new uranyl sulfate minerals from the Blue Lizard mine, San Juan County, Utah, USA. *Mineralogical Magazine*, **79**, 695–714.
- Kasatkin, A.V., Plášil, J., Belakovskiy, D.I. and Marty, J. (2014) Cobaltogordaite, IMA 2014-043. CNMNC Newsletter No.22, October 2014. *Mineralogical Magazine*, **78**, 1241–1248.
- Kraus, W. and Nolze, G. (1996) POWDER CELL – a program for the representation and manipulation of crystal structures and calculation of the resulting X-ray powder patterns. *Journal of Applied Crystallography*, **29**, 301–303.
- Lane, M.D. (2007) Mid-infrared emission spectroscopy of sulphate and sulphate-bearing minerals. *American Mineralogist*, **92**, 1–18.
- Libowitzky, E. (1999) Correlation of O–H stretching frequencies and O–H...O hydrogen bond lengths in minerals. *Monatshefte für Chemie*, **130**, 1047–1059.
- Mandarino, J.A. (1981) The Gladstone-Dale relationship: Part IV. The compatibility concept and its application. *Canadian Mineralogist*, **19**, 441–450.
- Merlet, C. (1994) An accurate computer correction program for quantitative electron probe microanalysis. *Microchimica Acta*, **114/115**, 363–376.
- Mills, S.J., Hatert, F., Nickel, E.H. and Ferraris, G. (2009) The standardisation of mineral group hierarchies: application to recent nomenclature proposals. *European Journal of Mineralogy*, **21**, 1073–1080.
- Nasdala, L., Witzke, T., Ullrich, B. and Brett, R. (1998) Gordaite $[\text{Zn}_4\text{Na}(\text{OH})_6(\text{SO}_4)\text{Cl}]\cdot 6\text{H}_2\text{O}$: second occurrence in the Juan de Fuca Ridge, and new data. *American Mineralogist*, **83**, 1111–1116.
- Sarp, H. (1993) Guarinoite $(\text{ZnCoNi})_6(\text{SO}_4)(\text{OH,Cl})_{10}\cdot 5\text{H}_2\text{O}$ et thérèsemagnanite $(\text{CoZnNi})_6(\text{SO}_4)(\text{OH,Cl})_{10}\cdot 8\text{H}_2\text{O}$,

- deux nouveaux minéraux de la mine de Cap Garonne, Var, France. *Archives des Sciences. Genève*, **46**(1), 37–44.
- Schlüter, J., Klaska, K.-H., Friese, K., Adiwidjaja, G. and Gebhard, G. (1997) Gordaite, $\text{NaZn}_4(\text{SO}_4)(\text{OH})_6\text{Cl}\cdot 6\text{H}_2\text{O}$, a new mineral from the San Francisco mine, Antofagasta, Chile. *Neues Jahrbuch für Mineralogie, Monatshefte*, 155–162.
- Thaden, R.E., Trites, A.F., Jr. and Finnell, T.L. (1964) *Geology and ore deposits of the White Canyon area, San Juan and Garfield Counties, Utah*. Bulletin, 1125. United States Geological Survey, Washington, D.C.